ELSEVIER

Thermochimica Acta 397 (2003) 181–197

thermochimica acta

www.elsevier.com/locate/tca

Ligand effects on the stability of some Mo(VI) and W(VI) peroxo complexes Part 2. Study of the thermal stability

Thokoza T. Bhengu, Dilip K. Sanyal*

Department of Chemistry, University of Fort Hare, Private Bag X1314, Alice, South Africa

Received 1 September 2001; received in revised form 7 May 2002; accepted 9 May 2002

Abstract

Twenty four peroxo complexes of Mo(VI) and W(VI) of the types (a) $K_2[MO(O_2)_2(L)]\cdot xH_2O$ where L = $C_2O_4^{2-}$, $C_4H_3O_4^{2-}$, $C_6H_6O_7^{2-}$, $C_4H_2O_4^{2-}$, $(OH)_2C_2H_2O_4^{2-}$ $NC_5H_7O_4^{2-}$, $NC_7H_3O_4^{2-}$ and $x = 0$ for $C_2O_4^{2-}$ and 1–2 for the rest and (b) $K_2[M_2O_2(O_2)_4(L')]$. xH_2O where $L' = C_3H_2O_4^{2-}$, $(OH)_2C_4H_2O_4^{2-}$, $NC_6H_4O_2^-$, $C_6H_4NO_3^-$, and $H_2NC_2H_2O_2^-$ and x = 1–4 were used to study thermal stability by both conventional heating as well as by thermogravimetry (TG), derrivative thermogravimetry (DTG) and differential scanning calorimetry (DSC). Decomposition temperatures of Mo(VI) complexes were found to be much higher than those of the corresponding W(VI) analogues. Peroxo complexes containing ligands having electron withdrawing functional group(s) decomposed explosively at temperatures lower than those without them. Decomposition reactions were established by mass loss, the peroxide content versus temperature, elemental analyses, and infrared (ir) spectroscopy.

Keywords: Glycinate; Ligand effect; Peroxide; Stability; Thermal analysis

1. Introduction

Part 1 of this investigation dealt primarily with the essential reaction conditions such as the stoichiometry, pH, temperature and the order of the addition of reagents for the synthesis of metal peroxo complexes in the most stable state. Twenty four complexes of Mo(VI) and W(VI) were prepared using various O- and N-donor ligands such as aspartate, dipicolinate, glutamate, glycinate, malonate, maleate, nicotinate, nicotinate N-oxide, oxalate and tartrate were involved in the establishment of the ideal synthetic conditions. In Part 2 of the present investigation, we report the effect of the donor sites, co-ordination geometry and the additional functional group(s) present in the ligands on the overall thermal stability of these complexes. The preliminary experiments on the stability studies were conducted by heating the solid complexes (a) in an atmosphere of oxygen free nitrogen and (b) under reduced pressure. Decomposition if any, was established from the loss of weight and the peroxide content, the elemental analyses and the infrared (ir) studies. Results of these studies were verified by the relevant instrumental techniques such as thermogravimetry (TG), derrivative thermogravimetry (DTG) and differential scanning calorimetry (DSC).

* Corresponding author. Fax: +27-40602-2366
E-mail address: dsanyal@ufh.ac.za (D.K. Sanyal).

0040-6031/02/$ – see front matter
PII: S0040-6031(02)00320-9

2. Experimental

Peroxo complexes of the type (a) $K_2[MO(O_2)_2(L)]\cdot xH_2O$, where M = Mo, W and L = $C_2O_4^{2-}$, $C_4H_3O_4^{2-}$, $C_6H_6O_7^{2-}$, $C_4H_2O_4^{2-}$, $(OH)_2C_4H_2O_4^{2-}$, $NC_5H_7O_4^{2-}$, $NC_7H_3O_4^{2-}$ and $x = 0$ for $C_2O_4^{2-}$ and 1–2 for the rest; (b) $K_2[M_2O_2(O_2)_4(L')]\cdot xH_2O$ where M = Mo, W and L′ = $C_3H_2O_4^{2-}$, $(OH)_2C_4H_2O_4^{2-}$, $NC_6H_4O_2^-$, $C_6H_4NO_3^-$ and $H_2NC_2H_2O_2^-$ where x = 1–4 have been prepared using the existing methods [1,2] with some modifications as described in Part 1. These are summarised later.

2.1. Complexes with O-donor ligands

An amount of 8.4 mmol of K_2MO_4 (2.0 g when M = Mo and 2.74 g when M = W) and the mass equivalent of 8.4 mmol of each ligand were dissolved in 10 cm^3 of distilled water. To the mixture 10 cm^3 of H_2O_2 (3% (v/v)) were added drop wise with constant stirring. Complexes were precipitated with 30 cm^3 ethanol, separated by filtration, washed with 3× 5 ml diethyl ether and air dried under a suction pump. For the dimeric complexes 16.8 mmol of K_2MO_4 and 8.4 mmol of the ligands were used.

2.2. Complexes with N-donor ligands

Same conditions as the O-donor ligands except that H_2O_2 was added to the aqueous solution of K_2MO_4 prior to the ligands (asp, $C_4H_3O_4^{2-}$; cit, $HOC_6H_5O_6^{2-}$; glu, $H_2NC_5H_5O_4^{2-}$; gly, $H_2NC_2H_2O_2^-$; mal, $C_3H_2O_4^{2-}$; malc, $C_4H_2O_4^{2-}$; nicH, $NC_6H_4O_2^-$; nicO, $C_6H_4NO_3^-$; ox, $C_2O_4^{2-}$; tart, $(OH)_2C_4H_2O_4^{2-}$ and dipic, $NC_7H_3O_4^{2-}$).

These complexes were analysed by conventional methods [3] (3a) as described in Part 1 and the results are summarised later as % content with the required values given in the parentheses.

Complexes—(1) $K_2[MoO(O_2)_2(ox)]$: C, 7.17 (7.01); O_2^{2-}, 18.94 (18.71); K, 22.53 (22.86); Mo, 28.16 (28.04). (2) $K_2[WO(O_2)(ox)]$: C, 5.69 (5.58); O_2^{2-}, 14.86 (14.88); K, 18.07 (18.18); W, 42.33 (42.75). (3) $K_2[MoO(O_2)_2$ (tart)]·$2H_2O$: C, 11.24 (10.95); H, 1.74 (1.83); O_2^{2-}, 14.41 (14.62); K, 13.89 (14.01); Mo, 21.20 (21.89). (4) $K_2[WO(O_2)_2$(tart)]·$2H_2O$: C, 8.84 (9.12); H, 1.31 (1.52); O_2^{2-}, 12.16 (12.16); K, 10.22 (10.48); W, 33.82 (34.34). (5) $K_2[MoO(O_2)_2(cit)]\cdot 3H_2O\cdot 0.5H_2O_2$: C, 11.01 (11.25); H, 2.09 (2.44); O_2^{2-}, 11.83 (12.00); K, 12.12 (12.03); Mo, 17.84 (17.99). (6) $K_2[WO(O_2)_2(cit)]\cdot 3H_2O\cdot 0.5H_2O_2$: C, 9.38 (9.66); H, 2.00 (2.09); O_2^{2-}, 9.92 (10.30); K, 9.12 (9.47); W, 28.84 (29.60). (7) $K_2[Mo_2O_2(O_2)_4$(tart)]·$4H_2O$: C, 7.29 (7.38); H, 1.77 (1.85); O_2^{2-}, 19.49 (19.69); K, 17.72 (17.84); Mo, 29.O_2 (29.51). (8) $K_2[W_2O_2(O_2)_4$ (tart)]·$4H_2O$: C, 5.62 (5.81); H, 1.01 (1.45); O_2^{2-}, 15.76 (15.50); K, 14.07 (14.86); W, 43.98 (44.52). (9) $K_2[MO_2O_2(O_2)_4$(mal)]·$2H_2O$: C, 6.34 (6.45); H, 0.90 (1.08); O_2^{2-}, 22.64 (22.53); K, 14.32 (14.66); Mo, 33.90 (34.38). (10) $K_2[W_2O_2(O_2)_4$(mal)]·$2H_2O$: C, 5.01 (4.83); H, 0.74 (0.80); O_2^{2-}, 17.32 (17.16); K, 12.82 (12.59); W, 48.96 (49.26). (11) $K_2[MoO(O_2)_2$ (malc)]·$2H_2O$: C, 11.12 (11.37); H, 1.72 (1.89); O_2^{2-}, 15.83 (15.16); K, 18.14 (18.52); Mo, 22.26 (22.72). (12) $K_2[WO(O_2)_2$(malc)]·$2H_2O$: C, 9.28 (9.41); H, 1.44 (1.57); O_2^{2-}, 12.22 (12.55); K, 14.89 (15.33); W, 35.92 (36.04). (13) $K_2[MoO(O_2)_2$(asp)]·$2H_2O$: C, 11.21 (11.39); H, 2.09 (2.14); N, 3.18 (3.32); O_2^{2-}, 14.97 (15.20); K, 18.42 (18.56); Mo, 21.63 (22.78). (14) $K_2[WO(O_2)_2$(asp)]·$2H_2O$: C, 9.12 (9.43); H, 1.62 (1.77); N, 2.33 (2.75); O_2^{2-}, 12.32 (12.57); K, 15.02 (15.36); W, 35.59 (36.11). (15) $K_2[MoO(O_2)_2$(glu)]·$2H_2O$: C, 13.21 (13.78); H, 2.17 (2.53); N, 3.03 (3.22); O_2^{2-}, 14.76 (14.70); K, 17.21 (17.97); Mo, 21.66 (22.04). (16) $K_2[WO(O_2)_2$(glu)]·$2H_2O$: C, 11.28 (11.74); H, 1.94 (2.10); N, 2.44 (2.68); O_2^{2-}, 12.02 (12.23); K, 14.39 (14.95); W, 35.66 (35.14). (17) $K_2[Mo_2O_2(O_2)_4$(nicH)]·H_2O: C, 11.88 (12.62); H, 1.34 (1.05); N, 2.95 (2.46); O_2^{2-}, 22.56 (22.45); K, 13.21 (13.71); Mo, 33.89 (33.65). (18) $K_2[WO(O_2)_2$(nicH)]·H_2O: C, 9.32 (9.65); H, 0.83 (0.80); N, 1.62 (1.88); O_2^{2-}, 16.98 (17.116); K, 10.84 (10.48); W, 48.92 (49.29). (19) $K_2[MO_2O_2(O_2)_4$(nicO)]·H_2O: C, 12.12 (12.28); H, 0.88 (1.02); N, 2.76 (2.39); O_2^{2-}, 22.20 (21.84); K, 13.42 (13.34); Mo, 33.11 (32.73). (20) $K_2[W_2O_2(O_2)_4$ (nicO]·H_2O: C, 9.82 (9.45); H, 0.88 (0.79); N, 2.13 (2.08); O_2^{2-}, 16.22 (16.80); K, 9.92 (10.36); W, 48.87 (48.25). (21) $K_2[Mo_2O_2(O_2)_4(gly)_2]\cdot 2H_2O$: C, 7.28 (7.82); H, 1.06 (1.30); N, 4.15 (4.56); O_2^{2-}, 20.19 (20.74); K, 12.24 (12.70); Mo, 30.97 (31.27). (22) $K_2[W_2O_2(O_2)_4(gly)_2]\cdot 2H_2O$: C, 4.67 (5.39); H, 0.93 (0.90); N, 3.09 (3.15); O_2^{2-}, 14.29 (14.38); K, 8.17 (8.76); W, 40.88 (41.35). (23) $K_2[MoO(O_2)_2$(dipic)]·H_2O: C, 18.77 (19.21); H, 1.24

(1.14); N, 2.95 (3.20); O_2^{2-}, 14.93 (14.64); K, 17.24 (17.88); Mo, 21.32 (21.94). (24) $K_2[WO(O_2)_2(dipic)]\cdot H_2O$: C, 16.16 (15.99); H, 1.07 (0.95); N, 2.29 (2.67); O_2^{2-}, 12.02 (12.19); K, 14.21 (14.89); W, 34.67 (35.01).

2.3. Preliminary stability studies

These experiments were carried out using a specially designed apparatus (see Fig. 1) for the thermal stability of the complexes in a stream of oxygen free dry nitrogen atmosphere. In these experiments changes involving (i) loss of mass versus temperature and (ii) the peroxide content versus temperature were studied according to the general procedure given later.

About 25 mg (∼150 mg for peroxide determinations) were evenly spread onto a pre-weighed shallow glass crucible. The crucible was then placed on a small Teflon coated tripod stand inside a 15 cm tall glass cylinder and the sample was heated to the desired temperatures for 60 min. The crucible was then covered with the lid and carefully transferred into a desiccator, cooled to room temperature before weighing and/or analysing for peroxide contents [3] (3b). The whole process was repeated at temperature intervals between 10 and 20 °C until no changes were observed. Similar studies were also repeated under reduced pressure, 1×10^{-1} mmHg using a glass vacuum manifold. Results from both set of experiments after 3–4 repetitions showed excellent agreements and these are given in Table 1. Elemental analyses of the decomposition intermediates/final products are given in Table 2a–c.

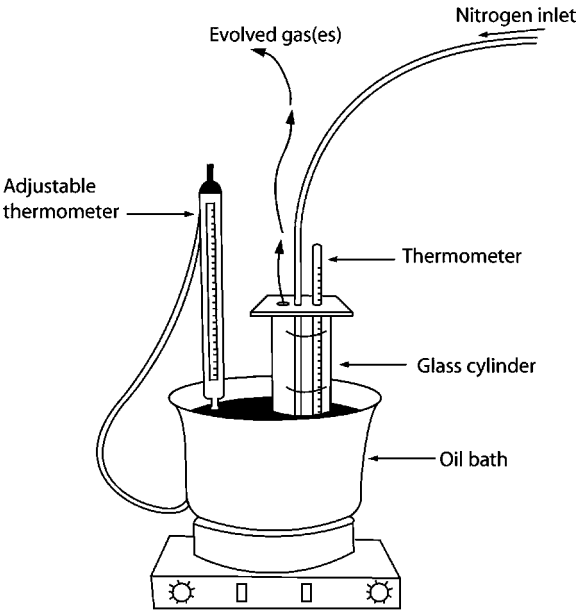

Fig. 1. Apparatus for preliminary stability study.

2.4. Confirmatory stability studies by instrumental methods

All thermal analysis experiments were carried out on a Perkin-Elmer Delta Series 7 TG and DSC. Very small samples (<2 mg) were used and samples were heated in open platinum pans (TG) and covered, but uncrimped, aluminium pans (DSC). The atmosphere was flowing nitrogen (60 $cm^3\,mm^{-1}$) The temperature scale of the DSC had been calibrated in normal fashion, using the melting points of indium and zinc metals, and the TG was calibrated using Curie points of Ni and Fe. To avoid ambiguity it is important to note that the DSC curves facing downwards (∨) are referred to "exothermic processes" and the "endothermic processes" are those facing upwards (∧). It should also be noted that these experiments could not be performed on all samples as some of these were found to damage the instruments.

3. Results and discussion

From the different set of experiments it has been observed that these complexes undergo varying modes of decomposition. Some complexes did, however, show certain similarities in their decomposition behaviours. Based on the similarities, these are grouped as follows.

Group A: These complexes undergo well defined decomposition pathways where in most cases the decomposition intermediates could be identified by chemical analysis and ir spectra. This group includes: oxalate, $K_2[MO(O_2)_2(ox)]$ (1 and 2); citrate, $K_2[MO(O_2)_2(cit)]\cdot 3H_2O\cdot 0.5H_2O_2$ (5 and 6) complexes.

Group B: These complexes undergo strongly exothermic decomposition which was evident from the spluttering of heated material inside the sample container. This group includes: malonate, $K_2[M_2O_2(O_2)_4(mal)]\cdot 2H_2O$ (9 and 10); tartarate

Table 1
Thermal decomposition of some of the peroxo complexes[a]

$K_2[MO(O_2)_2(ox)]$ (1 and 2)					$K_2[MO(O_2)_2(cit)]\cdot xH_2O\cdot yH_2O_2$ (5 and 6)				
Temperature (±2 °C)	Loss (wt.%)		O_2^{2-}		Temperature (±2 °C)	Loss (wt.%)		O_2^{2-}	
	Mo (1)	W (2)	Mo (1)	W (2)		Mo (5)	W (6)	Mo (5)	W (6)
30	0.0	0.0	18.9	–	30	0.0	0.0	11.8	9.9
40	0.0	0.0	–	14.8	40	0.0	0.0	11.8	9.9
50	0.2	–	18.9	–	50	0.0	0.0	11.1	9.6
60	0.4	0.14	–	14.6	70	1.9	10.3	10.6	8.4
70	0.4	–	18.7	–	90	3.6	13.4	10.0	6.9
80	0.4	0.0	–	14.4	100	7.3	–	9.1	–
90	0.4	–	18.5	–	110	–	18.3	–	5.2
100	0.6	1.1	18.4	13.4	120	9.4	–	8.2	–
110	0.6	–	18.3	–	130	–	21.1	–	3.1
120	0.6	1.1	–	13.3	140	9.9	–	7.4	–
130	1.4	2.9	18.0	12.1	150	–	22.1	–	2.5
140	4.1	6.2	16.9	8.9	160	10.7	–	7.1	–
150	4.6	–	13.3	–	170	–	23.0	–	0.92
160	7.3	11.5	11.7	1.6	180	11.8	–	6.6	–
170	10.2	12.9	10.1	0.9	190	–	23.7	–	0.0
180	10.4	13.1	9.1	0.0	200	14.8	–	3.8	–
190	–	–	–	–	210	17.1	25.5	2.1	0.0
200	10.8	13.2	6.9	0.0					
210	13.9	–	0.0	–					
$K_2[MO(O_2)_2(tart)]\cdot xH_2O$ (3 and 4)					$K_2[MO(O_2)_2(malc)]\cdot xH_2O$ (11 and 12)				
30	0.0	0.0	14.3	12.1	40	0.0	0.0	15.8	12.2
40	0.0	0.0	14.3	12.0	50	1.7	–	15.2	–
50	0.2	0.4	13.9	11.8	60	2.7	2.3	14.9	12.1
60	0.6	3.2	13.6	11.2	70	3.1	–	14.1	–
70	0.8	–	13.4	–	80	3.5	4.1	13.6	10.8
80	1.2	5.2	13.1	10.9	90	3.5	–	12.8	–
90	1.2	–	13.0	–	100	3.5	17.9	11.9	7.8
100	1.2	7.5	12.9	8.9	110	4.4	19.1	11.1	5.3
110	1.2	–	12.9	–	120	–	20.0	–	4.7
120	3.4	9.9	10.7	5.6	130	9.9	20.1	7.5	4.5
130	15.6	10.5	0.0	3.1	140	77.9	20.8	0.0	3.7
140	77.5	12.8	–	2.0	160	–	21.3	–	3.1
150	87.0	13.2	–	1.3	190	–	23.9	–	1.9
160	–	13.9	–	0.0	200	–	24.8	–	0.8
170	–	13.9	–	–	210	–	25.4	–	0.0
$K_2[M_2O_2(O_2)_4(gly)]\cdot xH_2O$ (21 and 22)					$K_2[MO(O_2)_2(asp)]\cdot xH_2O$ (13 and 14)				
40	0.0	0.0	23.1	17.6	40	0.6	0.0	14.0	12.2
50	0.5	0.0	22.9	17.5	50	3.3	3.3	10.1	9.2
60	1.5	2.4	22.5	16.9	60	8.3	7.4	8.9	8.2
70	1.7	2.9	20.9	16.4	80	9.5	7.4	8.6	8.1
80	1.9	3.7	18.8	16.1	100	12.8	8.3	6.9	7.8
90	2.5	3.9	16.9	15.7	120	15.1	21.9	4.3	2.4
100	2.9	4.1	16.4	15.1	140	23.8	66.1	2.9	0.9
110	–	5.3	–	13.8	160	29.5	66.2	0.0	0.5
120	6.7	8.8	10.8	10.3	180	–	66.5	–	0.2
130	59.6	73.8	0.9	0.9	200	–	66.9	–	0.0
140	72.9	74.0	0.0	0.0	210	–	–	–	–

Table 1 (*Continued*)

$K_2[MO(O_2)_2$ (g1u)]·xH_2O (15 and 16)					$K_2[M_2O_2(O_2)_4$(nicH)]·xH_2O (17 and 18)				
Temperature (±2 °C)	Loss (wt.%)		O_2^{2-}		Temperature (±2 °C)	Loss (wt.%)		O_2^{2-}	
	Mo (1)	W (2)	Mo (1)	W (2)		Mo (5)	W (6)	Mo (5)	W (6)
40	0.0	0.0	14.6	11.9	30	0.0	0.0	22.5	16.9
50	4.5	4.7	13.8	11.4	40	0.5	0.6	22.0	16.7
60	8.4	8.8	13.2	11.1	50	1.2	1.5	20.4	16.3
70	8.8	11.3	11.4	10.7	60	2.4	2.4	20.0	14.8
80	12.2	12.3	10.1	9.7	80	4.5	3.8	16.9	10.2
90	13.7	13.0	9.5	9.3	100	9.8	10.5	12.9	7.8
100	15.1	14.6	7.4	7.8	120	31.0	12.9	1.1	4.1
110	15.8	17.2	7.0	5.6	140	35.0	16.8	0.0	2.1
120	19.1	19.5	5.9	5.0	160	–	21.5	–	0.7
130	22.9	22.7	4.3	4.5	180	–	24.1	–	0.0
140	23.6	29.6	4.1	3.6	200	–	25.3	–	0.0
160	34.9	36.7	1.9	0.8	210	–	34.4	–	0.0
180	40.1	42.2	0.0	0.0		–		–	
$K_2[M_2O_2(O_2)_4$(nicO)]·xH_2O (19 and 20)					$K_2[MO(O_2)_2$(dipic)]·H_2O (23 and 24)				
30	0.0	0.0	22.1	16.2	30	0.0	0.0	14.9	12.0
40	0.0	0.6	22.0	16.1	40	0.0	0.9	14.8	11.8
50	1.4	1.5	21.7	16.0	50	1.3	1.5	14.2	11.0
60	2.4	2.4	20.8	15.3	60	5.3	4.1	13.2	10.2
70	3.7	3.8	19.1	15.1	70	8.2	6.3	12.7	9.9
80	3.7	10.0	18.7	13.3	80	11.6	9.4	11.4	8.7
100	4.1	11.5	16.9	13.1	100	15.0	12.4	9.3	6.4
120	7.8	12.9	12.3	12.7	120	16.6	16.6	6.2	3.2
140	11.9	15.0	8.4	8.5	140	16.8	16.8	3.6	2.1
160	21.6	21.4	3.2	5.5	160	17.5	18.8	2.1	0.9
180	23.0	24.1	0.0	1.8	180	19.6	19.4	0.0	0.0
200	25.9	32.4	0.0	0.0	200	22.1	38.5	0.0	0.0

[a] Loss (wt.%) and peroxo content versus temperature (odd numbers are the Mo and the even numbers are the corresponding W complexes).

monomer, $K_2[MO(O_2)_2$(tartl]·$2H_2O$ (3 and 4); dimer, $K_2[M_2O_2(O_2)_4$(tart)]·$4H_2O$ (7 and 8); maleate, $K_2[M_2O_2(O_2)_4$(malc)]·$2H_2O$ (11 and 12); glycinate, $K_2[M_2O_2(O_2)_4$(gly)] (21 and 22) complexes.

Explosive decomposition was found to be most common characteristic of all Mo complexes in this group. The corresponding W complexes, on the other hand with the exception of the glycinate decomposed at a slow rate.

Group C: Complexes in this group undergo initial decomposition through the loss of the co-ordinated H_2O molecule(s) followed by multistage decomposition with the formation of highly unstable intermediates. This group includes: aspartate, $K_2[MO(O_2)_2$(asp)]·$2H_2O$ (13 and 14); glutamate, $K_2[MO(O_2)_2$(glu)]·$2H_2O$ (15 and 16); nicotinate, $K_2[M_2O_2(O_2)_4$(nicH)]·H_2O (17 and 18); nicotinate N-oxide, $K_2[M_2O_2(O_2)_4$(nicO)]·H_2O (19 and 20); dipicolinate, $K_2[MO(O_2)_2$(dipic)]·H_2O (23 and 24) complexes. It is to be noted that in the above pairs of complexes, the odd number refers to Mo while the even ones are the corresponding W complexes.

Infrared spectra of all solid samples, pure and the decomposition products were recorded on a Pye-Unicam SP3-300S spectrophotometer as mulls in liquid paraffins between AgCl windows or as KBr discs. Significant ir frequencies with the probable assignments [2,4–9] are given in Table 3 for the pure complexes and in Table 4a–c for the decomposition products.

Table 2
Analysis of decomposition intermediates products of the peroxo complexes of Mo (odd numbers) and W (even numbers)

Complex number	Temperature range (°C)	%C	%H	%N	%M	$\%O_2^{2-}$
(a) Oxalato (1 and 2) and citrato (5 and 6) complexes						
1	190–195	7.80 (7.17)	0.38	–	32.60 (28.16)	9.76 (18.94)
2	180–185	5.01 (5.69)	0.38	–	45.50 (42.33)	0.0 (14.86)
5	140–145	14.9 (11.01)	1.34 (2.09)	–	17.80 (17.84)	11.88 (11.83)
	200–210	12.22	1.25	–	20.90	6.37
6	140–145	<0.3 (9.38)	0.39 (2.00)	–	61.20 (28.84)	3.05 (9.92)
	180–185					
(b) Malete (9 and 10), tartrate monomer (3 and 4) tartrate dimer (7 and 8), maleate (11 and 12) and glycinate (21 and 22) complexes						
9	150–155	<0.03 (6.34)	<0.3 (0.9)	–	37.10 (33.90)	0.0 (22.64)
10	150–155	<0.3 (5.01)	0.48 (0.74)	–	60.80 (48.96)	2.69 (9.92)
	180–185	<0.3	0.59	54.80	–	0.0
3	130–135	3.83 (11.24)	<0.3 (1.74)	–	34.30 (21.20)	0.0 (14.41)
4	180–185	1.59 (8.84)	<0.3 (1.31)	–	51.80 (33.82)	0.0 (12.16)
7	130–135	2.14 (7.29)	<0.3 (1.77)	–	33.50 (29.02)	0.0 (19.49)
8	195–200	0.57 (5.62)	<0.3 (1.01)	–	57.40 (43.98)	0.0 (15.76)
11	170–175	4.01 (11.12)	<0.3 (1.72)	–	38.80 (22.26)	0.0 (15.83)
12	125–130	–	–	–	36.12 (35.92)	4.70 (12.22)
	200–205	–	–	–	40.29	2.00
21	See Section 3 for details					
22	75–80	–	–	1.72 (1.77)	50.94 (50.88)	17.72 (17.62)
(c) Aspartate (15 and 16), glutamate (17 and 18), nicotinate (19 and 20), nicotinate N-oxide (21 and 22) and dipicolinate (23 and 24) complexes						
15	240–250	–	–	2.74 (3.18)	35.35 (21.63)	0.0 (14.97)
16	205–210	–	–	2.19 (2.33)	48.20 (35.59)	0.0 (12.32)
17	150–155	14.0 (13.21)	<0.3	2.83 (3.03)	32.10 (21.88)	0.0 (14.76)
18	190–200	–	–1.82 (2.44)	56.22 (35.66)	0.0 (12.02)	
19	105–110	6.08 (11.88)	1.09 (1.34)	1.09 (2.95)	20.41 (33.89)	4.42 (22.56)
20	190–200	–	–	2.42 (1.62)	59.12 (48.92)	5.55 (16.98)
21	100–110	–	–	3.27 (2.76)	39.20 (33.11)	6.17 (22.20)
22	185–200	–	–	2.52 (2.13)	59.62 (48.87)	4.84 (16.22)
23	150–155	20.2 (18.77)	0.83 (1.24)	3.22 (2.95)	20.80 (21.32)	1.72 (14.93)
24	130–135	–	–	2.18 (2.28)	34.82 (34.67)	3.00 (12.02)

It is evident from the infrared data in Table 4a–c that all decomposition products including those of the oxalato complexes show broad band in the frequency range 3600–3200 cm^{-1}, characteristic of the –OH vibration [9]. This is an indication that these products are highly moisture sensitive and readily pick up some H_2O molecule(s) from the atmosphere. Details of the complex behaviour are discussed under each group.

Group A: $K_2[MO(O_2)_2(ox)]$ (1 and 2) and $K_2[MO(O_2)_2(cit)]\cdot 3H_2O\cdot 0.5H_2O_2$ (5 and 6) (Tables 2a and 4a).

The TG and DTG curves in Fig. 2a of Mo-oxalato complex (1) show that no weight loss is associated with 1 up to 180 °C, while in the temperature range 180–269 °C this complex undergoes two stage decomposition as confirmed by the presence of two peaks at 230 and 256 °C. The corresponding W complex (2) on the other hand, undergoes a single stage decomposition in the region 200–237 °C (see Fig. 2b). Elemental analysis in Table 2a as well as the ir data in Table 4a suggest that complex 1 loses one peroxo group at 180–230 °C forming a very unstable and

Table 3
Significant infrared frequencies (ν, cm^{-1}) of the of the peroxo complexes with probable assignments[a,b]

Complex number	Complex	ν[M=O]	ν[O–O]	$\nu_{asy}[M(O)_2]$	$\nu_{sym}[M(O)_2]$	$\nu_{asy}[CO_2M]$
1	$K_2[MoO(O_2)_2(ox)]$	972 (s) 906 (w)	874 (s) 800 (s)	660 (s) 588 (s)	534 (m) 518 (m)	1672 (s, br)
2	$K_2[WO(O_2)_2(ox)]$	981 (vs) 918 (w)	854 (s) 806 (s)	655 (s) 594 (m)	530 (s)	1685 (s, br)
3	$K_2[MOO(O_2)_2(tart)]\cdot 2H_2O$	956 (vs) 920 (w)	870 (w) 854 (vs)	648 (s) 640 (w, br)	580 (s)	1580 (s)
4	$K_2[WO(O_2)_2(tart)]\cdot 2H_2O$	960 (s)	852 (m) 838 (m)	 650 (s)	555 (w, br)	1636 (m)
5	$K_2[MOO(O_2)_2(cit)]\cdot 3H_2O\cdot 0.5H_2O_2$	946 (s) 972 (vs)	875 (m) 858 (s)	614 (m) 620 (w)	562 (m) 500 (s)	1595 (s, br)
6	$K_2[WO(O_2)(cit)]\cdot 3H_2O\cdot 0.5H_2O_2$	956 (vs) 920 (s)	842 (s)	644 (s) 648 (w, br)	550 (s, br)	1596 (s, br)
7	$K_2[MO_2O_2(O_2)_4(tart)]\cdot 4H_2O$	955 (s) 963 (s)	870 (m) 854 (s)	620 (w) 668 (w)	575 (s)	1594 (s, br)
8	$K_2[W_2O_2(O_2)_4(tart)]\cdot 4H_2O$	928 (s) 970 (s)	862 (w) 842 (m)	 615 (m)	536 (w, br)	1640 (s, br)
9	$K_2[Mo_2O_2(O_2)_4(mal)]\cdot 2H_2O$	951 (vs) 915 (m)	868 (s) 850 (m)	 619 (m)	572 (m) 528 (w)	1640 (s, br)
10	$K_2[W_2O_2(O_2)_4(mal)]\cdot 2H_2O$	969 (vs) 960 (m)	860 (m) 840 (s)	 647 (w)	556 (s, br) 580 (m)	1640 (s, br)
11	$K_2[MoO(O_2)_2(malc)]\cdot 2H_2O$	902 (w) 972 (m)	862 (s) 839 (s)	 645 (s)	512 (m) 545 (s, br)	1578 (s, br)
12	$K_2[WO(O_2)_2(malc)]\cdot 2H_2O$	901 (w)	 853 (s)	647 (w)	570 (m)	1636 (m)
13	$K_2[MoO(O_2)_2(asp)]\cdot 2H_2O$	969 (vs)	 840 (m)	 660 (w)	555 (m)	1600 (m, br)
14	$K_2[WO(O_2)_2(asp)]\cdot 2H_2O$	960 (m) 902 (w)	859 (m) 819 (w)	625 (w) 619 (w)	 578 (m)	1609 (m)
15	$K_2[MoO(O_2)_2(glu)]\cdot 2H_2O$	970 (s) 966 (s)		 633 (w)	 539 (m)	1644 (m)
16	$K_2[WO(O_2)_2(glu)]\cdot 2H_2O$	978 (s)		618 (m)	578 (m)	1642 (m)
17	$K_2[Mo_2O_2(O_2)_4(nicH]\cdot H_2O$	958 (s)	864 (s)	577 (s)	556 (s, br)	1664 (m)
18	$K_2[W_2O_2(O_2)_4(nicH]\cdot H_2O$	972 (s)	840 (s)	620 (w)	528 (w)	1636 (m)
19	$K_2[MO_2O_2(O_2)_4(nicO)]\cdot H_2O$	942 (s)	862 (s)		545 (s, br)	1678 (m)
20	$K_2[W_2O_2(O_2)_4(nicO)]\cdot H_2O$	951 (vs) 970 (w)	841 (s)		552 (m)	1639 (m)
21	$K_2[Mo_2O_2(O_2)_4(gly)]\cdot 2H_2O$	970 (m) 951 (w)	865 (s)	 622 (m)	562 (s)	1622 (s)
22	$K_2[W_2O_2(O_2)_4(gly)]\cdot 2H_2O$	968 (s) 955 (w)	851 (s)	 655 (w)	538 (s)	1620 (s)
23	$K_2[MoO(O_2)_2(dipic)]\cdot H_2O$		802 (vs)	 652 (w, br)	550 (w, br)	1640 (m)
24	$K_2[WO(O_2)_2(dipic)]\cdot H_2O$		862 (w) 840 (w)		541 (w, br)	1638 (m)

[a] Notation: vs, very strong; s, strong; m, moderate; sh, shoulder; w, weak; br, broad.
[b] ν(OH) for co-ordinated H_2O were found as weak and broad band at 3200–3600 cm^{-1}.

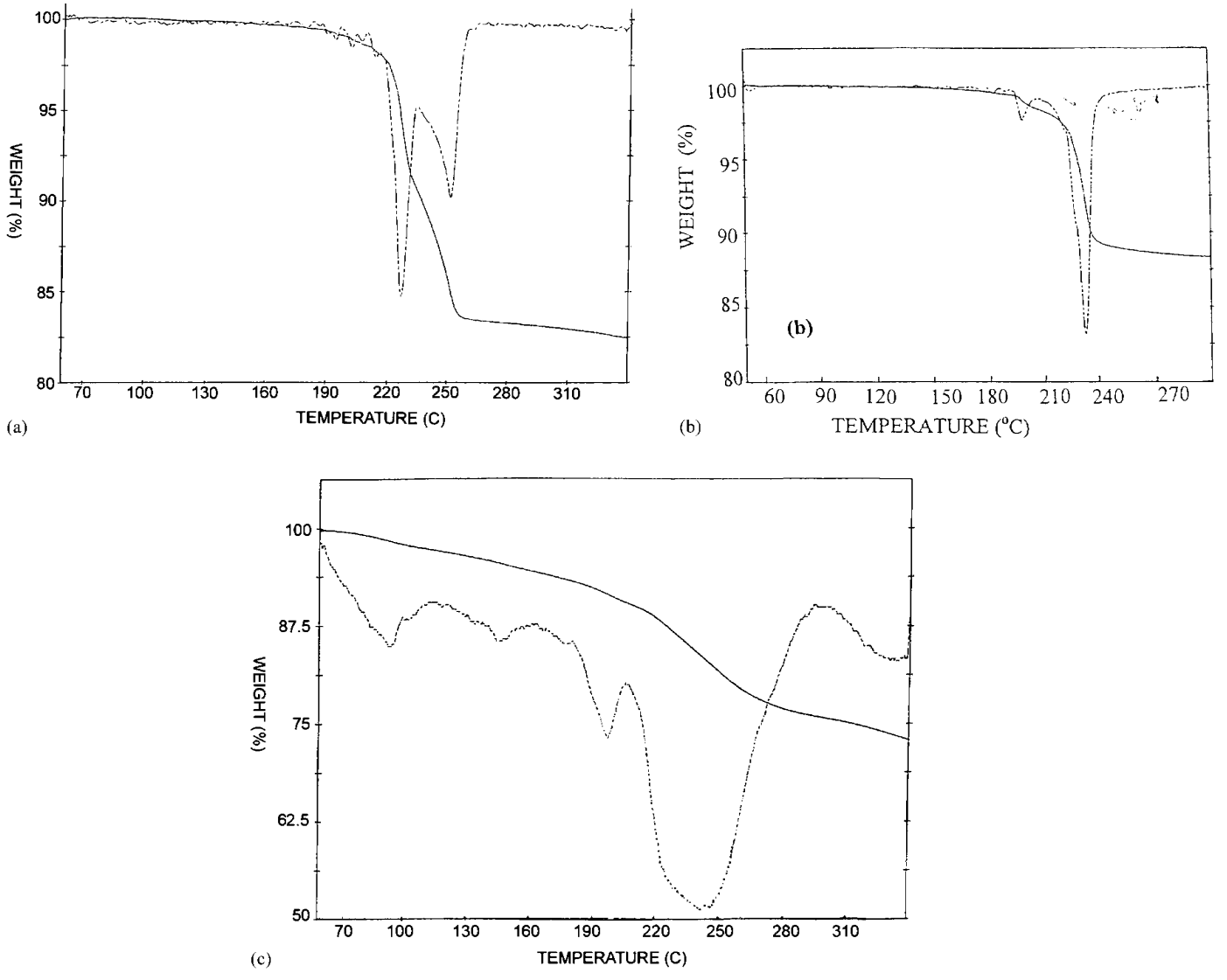

Fig. 2. TG and DTG plot of (a) $K_2[MoO(O_2)_2(ox)]$; (b) $K_2[WO(O_2)_2(ox)]$; (c) $K_2[MoO(O_2)_2(asp)_2]\cdot H_2O$.

Table 4
Significant infrared frequencies (ν, cm^{-1}) of the decomposition products/intermediates of the Mo (odd numbers) and W (even numbers) peroxo complexes

Complex number	Temperature range (°C)	ν[M=O]	ν[O–O]	$\nu_{asy}[M(O)_2]$	$\nu_{sym}[M(O)_2]$	$\nu_{sym}[CO_2M]$, ν[C=O]	ν(OH)
(a) Oxalato (1 and 2) and citrato (5 and 6) complexes							
1	190–195	946 (m) 890 (s)	800 (m)	520 (w)	484 (w)	1660 (s, br)	3430 (m, br)
2	180–185	946 (m) 898 (m)	–	–	–	1650 (s, br)	3416 (m, br)
5	140–145	945 (s)	875 (m) 860 (s)	649 (s) 614 (m)	561 (m) 502 (m)	1640 (s, br)	3321 (m, br)
	200–210	922 (m, br) 890 (m)	845 (w)	–	–	1578 (m, br)	3349 (m, br)
6	140–145	942 (w) 890 (w)	–	–	–	1532–1730 (w, br)	3290 (w, br)
	180–185	940 (w) 880 (w)	–			1540–1730 (w, br)	3294 (m, br)
(b) Malete (9 and 10), tartrate monomer (3 and 4), tartrate dimer (7 and 8), maleate (11 and 12) complexes							
9	150–155	800–9009 (s, br)	–	–	–	1640 (w, br)	3400 (w, br)
10	150–155	930 (s)	887 (w)	–	–	1630 (m, br)	3250 (m, br)
	180–185	928 (s)	–	–	–	1630 (m, br)	3450 (m, br)
3	130–135	834 (s, br)	–	–	–	1639 (w, br)	3400 (w, br)
4	180–185	922 (sh)	879 (w)	–	–	1630 (s, br)	3500 (w, br) 912 (s)
7	130–135		842 (vs)	–	–	1642 (vs)	3450 (w, br)
8	195–200	940 (m)	890 (s)	–	–	1645 (s, br)	3400 (w, br)
11	170–175	828 (s)	–	–	–	1625 (w, br)	3450 (w, br)
12	125–130	936 (m)	885 (m)	–	–	1620 (m, br)	3400 (w, br)
	200–205	935 (m)	885 (sh)	–	–	1625 (w, br)	3400 (w, br)
(c) Aspartate (13 and 14), glumamate (15 and 16), nicotinate (17 and 18), nicotinate N-oxide (19 and 20), and dipicolinate (23 and 24) complexes							
13	240–250	926 (m) 901 (m)	–	–	–	1572 (w, br)	3400 (w, br)
14	205–210	918 (m) 894 (m, br)	–	–	1538 (w, br)	3450 (w, br)	
15	150–155	892 (m, br)	–		–	1640 (m, br)	3400 (w, br)
16	190–200	945 (m)	–	–	–	1650 (s, br)	3400 (w, br)
17	105–110	907 (m)	802 (w)	–	–	1617 (w, br)	3350 (w, br)
19	190–200	933 (m)	–	–	–	1633 (w, br)	3350 (w, br)
19	100–110	849 (m)	–	–	–	1632 (w, br)	3400 (w, br)
20	190–195	912 (m)	–	–	–	1635 (w, br)	3450 (w, br)
23	150–155	932 (m)	871 (w)	–	–	1645 (w, br)	3450 (w, br)

highly moisture sensitive oxomonoperoxo Mo(IV) complex, reduction of M(VI) to M(IV) also finds support from the literature report [10]. $K_2[MoO(O_2)(ox)]$ which immediately picks up some atmospheric water forming $K_2[MoO(O_2)(ox)]\cdot 0.5H_2O$ (1a). Elemental analysis, found %Mo, 32.60; %C, 7.80; %H, 0.38 and $\%O_2^{2-}$, 9.76 and those required for 1a, $K_2[MoO(O_2)(ox)]\cdot 0.5H_2O$: %Mo, 30.06; %C, 7.52;

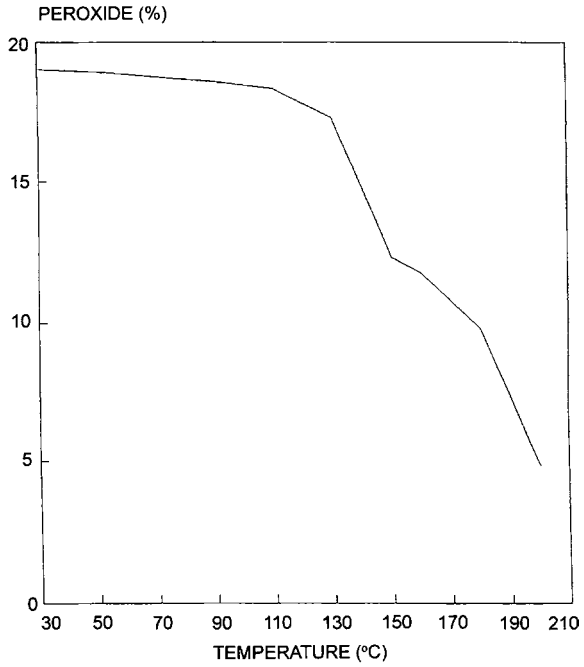

Fig. 3. TG plot of peroxide vs. temperature for $K_2[MoO(O_2)_2(ox)]$.

%H, 0.31; $\%O_2^{2-}$, 10.03 and also presence of the vibration band at 3430 cm^{-1}, characteristic of ν(OH) are quite agreeable with the proposed formulation of the hydrated intermediate as described by 1a. Formation of the intermediate 1a through the loss of H_2O_2 is also evidenced from the TG plot of peroxide content versus temperature as shown in Fig. 3. The second peak for 1 found at 256 °C presumably the result of decarboxylation of the oxalato group. This assumption is supported by number reports [11–14] that decarboxylation of peroxy carboxylato complexes of Mo actually takes place in the temperature range 225–300 °C. Two exothermic peaks in the DSC curve of heat flow versus temperature as shown in Fig. 4a provide further evidence in support of both the decomposition and the decarboxylation (only one TG and DTG curve per group is included, rest are available on request).

In case of W complex (2) peroxide is lost completely when it is isothermally heated at 180–185 °C. This is evidenced from complete absence of the peroxo vibration frequency and the chemical analysis. The TG curve of peroxide content versus temperature also confirm this observation. Presence of an absorption band at 3416 cm^{-1} characteristic of ν(OH) vibration result from the fact that the decomposition intermediate of 2, $K_2[WO_3(ox)]$, being highly moisture sensitive readily forms $K_2[WO_3(ox)]\cdot H_2O$ (2a) when exposed to the atmosphere. Analytical data with the required values in the parenthesis: %W, 45.50 (44.19); %C, 5.01 (5.77); %H, 0.38 (0.48); $\%O_2^{2-}$, 0.0 (0.0), are in fair agreement with this conclusion. The intermediate 2a undergoes further decomposition in the temperature range 200–230 °C which like the Mo complex is the result of decarboxylation. The decarboxylation of 2a is a strongly exothermic process occurring at 221.26 °C (see DSC curve in Fig. 4b) with the enthalpy change, $\Delta H = -190 \pm 10\ kJ\ mol^{-1}$. On the basis of the experimental evidence the decomposition process of the two oxalato systems are shown by the following reactions.

Mo complex (1):

$$\underset{(1)}{K_2[MoO(O_2)_2(C_2O_4)]} \xrightarrow[N_2\ (g)\ flow]{180–230\ ^\circ C} \underset{(1a)}{K_2[MoO(O_2)(C_2O_4)]} + 2(O)$$

$$\underset{(1a)}{K_2[MoO(O_2)(C_2O_4)]} \xrightarrow[N_2\ (g)\ flow]{230–269\ ^\circ C} \underset{(1b)}{K_2[MoO_3]} + 2CO_2$$

W complex (2):

$$\underset{(2)}{K_2[WO(O_2)_2(C_2O_4)]} \xrightarrow[N_2\ (g)\ flow]{180\ ^\circ C} \underset{(2a)}{K_2[WO_3(C_2O_4)]} + 2(O)$$

$$\underset{(2a)}{K_2[WO_3(C_2O_4)]} \xrightarrow[N_2\ (g)\ flow]{237\ ^\circ C} \underset{(2b)}{K_2[WO_3]} + 2CO_2$$

For the citrato complexes $K_2[MO(O_2)_2(cit)]\cdot 3H_2O\cdot 0.5H_2O_2$ (5 and 6), analytical results in Table 2a and the TG and DTG curve suggest that the Mo complex (5) undergoes two stage decompositions, one at 140–145 °C and the other at 200–210 °C. DSC curve of 5 (see Fig. 4c), however, shows a four stage decomposition, the first one an endothermic process ($\Delta H = 276 \pm 10\ kJ\ mol^{-1}$) occurring at 123 °C This is believed to be associated with the loss of the outer sphere peroxide, forming the trihydrate $K_2[MoO(O_2)(cit)]\cdot 3H_2O$ (3a). Analytical results of this species, with the calculated values in the parentheses: %Mo, 17.80 (18.58); %C, 14.99

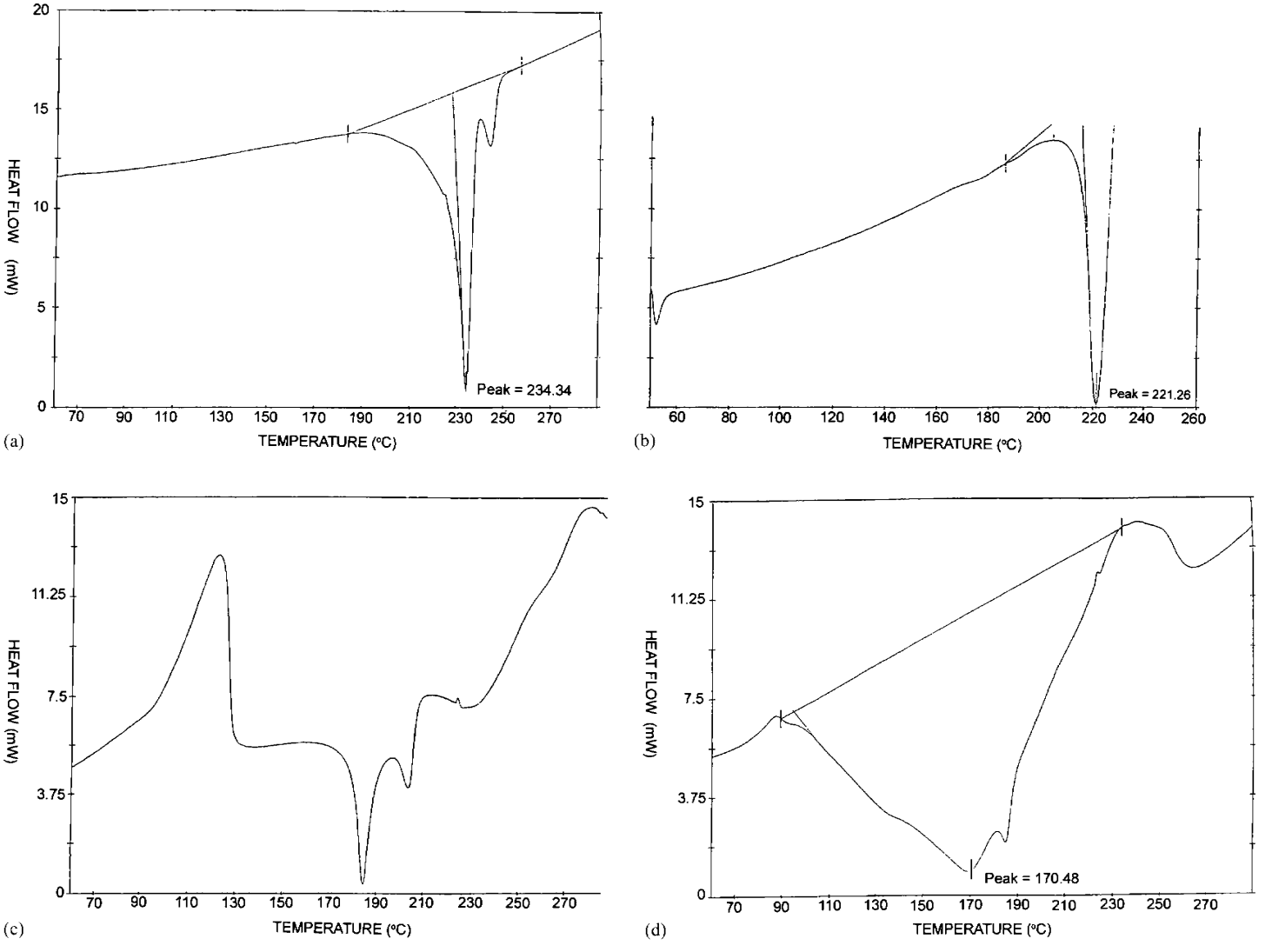

Fig. 4. DSC plot of heat flow vs. temperature for (a) $K_2[MoO(O_2)_2(ox)]$; (b) $K_2[WO(O_2)_2(ox)]$; (c) $K_2[MoO(O_2)_2(cit)]\cdot 3H_2O\cdot 0.5H_2O_2$; (d) $K_2[MoO(O_2)_2(asp)]\cdot 2H_2O$.

(13.96); %H, 1.34 (2.32); and $\%O_2^{2-}$, 11.88 (12.40) and the observed mass loss (found 3.14% and that required for 5a is 3.19%) are also in good agreement with this assumption. This intermediate is fairly stable up to 200 °C and above this temperature further decomposition occurs resulting in the formation of highly unstable product. It is suggested that 5a first undergoes complete dehydration at 200–220 °C followed by the rearrangement of the crystal lattice through an exothermic process as confirmed by the TG and DTG plot resulting an anhydrous species $K_2[MoO_2(O_2)(cit)]$ (3b). The net enthalpy change for the process, $\Delta H = -136 \pm 10\,kJ\,mol^{-1}$. Like the oxalato complexes this intermediate also being moisture sensitive is readily gets hydrated forming $K_2[MoO_2(O_2)(cit)]\cdot H_2O$. Thermal decomposition and the rearrangement of the crystal lattice of the Mo complex (5) is given by the following reactions.

$$\underset{(5)}{K_2[MoO(O_2)_2(cit)]\cdot 3H_2O\cdot 0.5H_2O_2} \xrightarrow[N_2\,(g)]{50\text{–}120\,^\circ C} \underset{(5a)}{K_2[MoO(O_2)(cit)]\cdot 3H_2O} + 0.5H_2O + 0.5O_2$$

$$\Delta H = 276 \pm 10\,kJ\,mol^{-1}$$

$$\underset{(5a)}{K_2[MoO(O_2)_2(cit)]\cdot 3H_2O} \xrightarrow[200\text{–}220\,^\circ C]{\text{dehydration/rearrangement}} \underset{(5b)}{K_2[MoO(O_2)(cit)] + 2O} + 3H_2O$$

$$\Delta H = -136 \pm 10\,kJ\,mol^{-1}$$

The intermediate 5b undergoes extensive decomposition at temperatures 285–300 °C forming the oxomolybdate (5c) and carbonacious matters as shown later.

$$\underset{(5b)}{K_2[MoO(O_2)(cit)]} \xrightarrow[N_2\,(g)]{285\text{–}300\,^\circ C} K_2[MoO_x] + Z \quad (5c)$$

where $x = 3$–4, Z = carbonacious matters.

From the experimental observations, it is evident that the distortion of the inner sphere structure in Group A complexes results from the rupture of the O–O bonds and not from (M–O) bonds of the M–L co-ordination. This behaviour may be attributed to the fact that both the oxalate $(COO^-)_2$ and the citrate $[(CH_2COO^-)_2COHCOOH]$ ligands not having electron withdrawing functional groups would result in the strengthening of the M–L bonds. The O–O bonds, on the other hand, remains relatively weak and are readily affected at higher temperature. Evidence from both the ir spectra and the TG plot support the loss of O_2^{2-} at elevated temperatures. It is also observed that the decomposition temperatures of all W complexes in this group are lower than those of the corresponding Mo analogues. This behaviour is the result of the electrostatic interaction between M^{6+} and O_2^{2-} which is weaker for the W complexes due to larger size of the W^{6+}-ion.

Group B: $K_2[M_2O_2(O_2)_4(mal)]\cdot 2H_2O$ (9 and 10); $K_2[MO(O_2)_2(tart)]\cdot 2H_2O$ (3 and 4); $K_2[M_2O_2(O_2)_4(tart)]\cdot 4H_2O$ (7 and 8); $K_2[MO(O_2)_2(malc)]\cdot 2H_2O$ (11 and 12); $K_2[M_2O_2(O_2)_4(gly)]\cdot 4H_2O$ (21 and 22).

The malonate complex of Mo (9) is stable up to 210 °C but forms a black solid (9a) above this temperature through explosive decomposition. TG plot of wt.% loss versus temperature (see Fig. 5A) and the analytical result in Table 2b indicate that the decomposition is associated with a very sharp loss of mass and complete absence of peroxide in the black residual solid. The corresponding W complex (10) on the other hand, undergoes slow decomposition in the temperature range 61–155 °C with the constant loss of mass and the peroxide content resulting in a very unstable compound (10a), which undergoes further dissociation in the temperature range 170–200 °C. Peroxide content of 10a was found to be 2.69% compared to 17.32% in the pure sample (10). From the experimental evidence including the weakening of the O_2^{2-} vibration frequency at 887 cm^{-1} it may be concluded that the loss of peroxide is the main reason for the weight loss observed at this stage. Since 10a is extremely unstable and moisture sensitive the stoichiometry of this product is uncertain. However, chemical analysis of the product at 180–185 °C was found to contain %W, 54.85; %H, 0.59; $\%O_2^{2-}$, 0.0 which matches closely to that required (%W, 55.05; %H, 0.60; $\%O_2^{2-}$, 0.0) for $K_2[W_2O_4(mal)]\cdot H_2O$. The observed mass loss of 17.35% compared to the expected value of 17.70% also provide further evidence in support of the composition as formulated earlier.

The monomeric tartrate complex of Mo (3) follows the same decomposition pattern as the corresponding malonate complex 9 since both decompose explosively at the maximum temperature. The decomposition of 3 results in a sharp loss of mass as confirmed by the

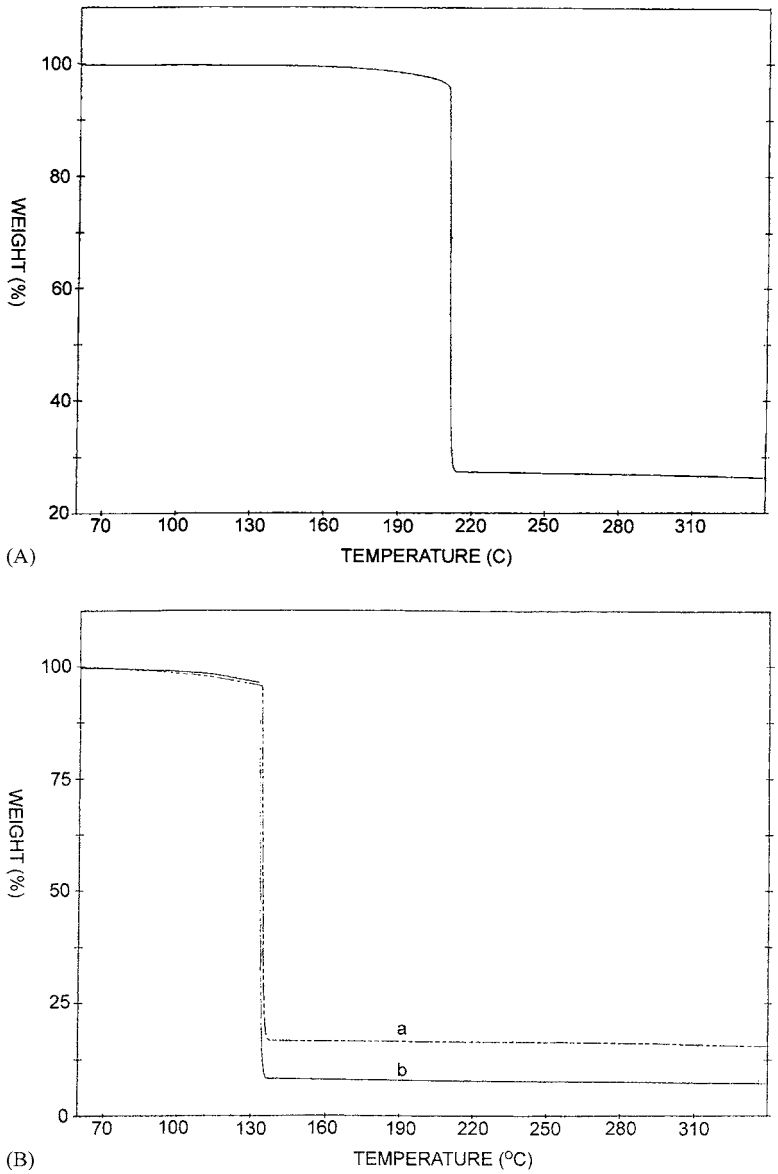

Fig. 5. TG plot of wt.% loss vs. temperature for (A) $K_2[Mo_2O_2(O_2)_4(mal)]\cdot 2H_2O$; (B) $K_2[MoO(O_2)_2(tart)]\cdot 2H_2O$ (a), $K_2[Mo_2O_2(O_2)_4(tart)]\cdot 4H_2O$ (b).

TG curves. Analytical results of C and H in this decomposition product are 3.83 and <0.3%, respectively compared to the corresponding values of 11.24 and 1.74% found in the pure complex. Again the observed ir frequency at 1679 cm^{-1} assignable to $\nu(CO_2M)$ is at a considerably higher energy than that found in the pure sample. These findings are agreeable with the suggestion that the Mo-tartrate chelate ring suffers complete distortion of the higher co-ordination geometry during the decomposition resulting in a product of uncertain composition. The corresponding tungsten complex 4 follows similar decomposition pathways

as the other W complexes, decomposing slowly with the increasing temperature. This is evidenced from TG and DTG plot of wt.% loss versus temperature. Analytical results of the product at 180–185 °C (see Table 2b) show very low C and H content, 1.59 and <0.3%, respectively compared to the corresponding values of 8.84 and 1.31% in the pure complex. The low C and H content may be the consequence of some degree of decomposition of the ligand itself. As stated earlier due to high degree of unstability identity of this product is also uncertain. The tartrate dimers (7 and 8) follow similar decomposition pattern as those of the monomers (3 and 4). Here the Mo complex 7 undergoes explosive decomposition at ∼135 °C resulting in a dark grey residual solid with very low C and H content as shown in Table 2b. The ir spectra of the decomposition product of 7 confirms the presence of two vibration bands in the region 840–920 cm^{-1} which are characteristic of the oxo ligand *cis* to the metal ion [14] and some reports claim also that the oxo attachments are of μ type [15,16], this asymmetry finds support from the slight lowering of the observed ν(M=O) as compared to the pure complexes. However, due to reasons stated earlier it was not possible to characterise this product. The W complex (8) decomposes to a brown solid at 195–200 °C. Evidence from the analytical results and the ir frequencies do confirm the presence of oxo-tungsten and the carbonyl species in the brown solid. Although the analytical results in Table 2b are not conclusive enough to suggest the true composition of the products, the colour changes of both 7 and 8 on decomposition do indicate reduction of these M^{6+} species to some lower oxidation states as explained for the Group A complexes.

For the Mo-maleate complex (9) TG plot confirms that the complex undergoes explosive decomposition at 175 °C forming a dark grey solid. Chemical analysis (see Table 2b) and the ir data (see Table 4b) are consistent with the assumption that this decomposition intermediate is an Mo-oxo species with the probable formula $K_2[MoO_4]\cdot 0.5H_2O$ (9a) as the observed Mo content (38.80%) is close enough to that required (38.82%) for 9a. Decomposition of the W-analogue (10) on the other hand, starts at temperatures just over 50 °C. The TG plot of wt.% loss versus temperature (Table 1) also supports the fact that the decomposition takes place through the formation of two fairly stable states, one at 120–140 °C and the other at ∼200 °C. Although the elemental analysis (see Table 2b) and the observed vibration frequencies at 935, 885 and 1710 cm^{-1} assignable to ν(M=O), ν(O–O) and $\nu(CO_2M)$, respectively confirm the presence of traces of O_2^{2-} in the product its true composition is still inconclusive.

In case of the glycinate system, the Mo complex (21) is fairly stable up to 195 °C above which it undergoes violent decomposition leaving no residual solid. The TG plot confirms this observation. The W-analogue (22) also behaves in a similar manner but the decomposition occurs at a much lower temperature of ∼130 °C. This is confirmed by the TG plot.

All Mo complexes in this group decompose explosively at the maximum temperature, which was found at 210 °C for the malonate, 135 °C for both monomeric and dimeric tartrate (see Fig. 2b) and 160 °C for the maleate system. This trend supports the view that the presence of electron withdrawing functional groups as well as the weakness of donor ligand causes destabilising effect on the M–O or even the $[M(O)_2]$ bonds. It is expected that the ligands without any additional electron withdrawing functional groups would form stronger M–O bonds than those containing these. The later being electron withdrawal in nature is expected to weaken the M–O and the $M(O_2)_2$ linkages. This theory is supported by the results of the thermal analysis which confirm that the malonate ligand, $^{-}OOC–CH_2COO^{-}$, having no additional functional groups such as –OH has the highest decomposition temperature (210 °C). In the case of the respective maleate, $^{-}OOC–CH_2CH(OH)–COO^{-}$, and the tartrate –OOC–CH(OH)–CH(OH)–COO–, ligands with one and two additional –OH groups, respectively decomposition of the complexes take place at much lower temperatures which were found at 160 °C for the maleate and 135 °C for the tartrate systems. The fact that both the monomeric and the dimeric tartrato complexes undergo bond rupture at the same temperature suggest that the complex decomposition is independent of the co-ordination geometry but the process is strongly influenced by the nature of the chelating organic ligands. Thermal analyses also reveal that like the Group A, W complexes of Group B do not undergo explosive decomposition

but suffers increasing mass loss with increased temperatures. The lower decomposition temperatures for the W complexes should follow similar argument as that for the Group A complexes.

The bond rupture of the metal peroxo and the metal carboxylato species proceeds steadily with increasing temperature which is supported by the observation that no stable intermediates were formed when the W complexes are subjected to higher temperatures. In the case of the glycinate complexes, an additional peak at ∼540 cm^{-1}, characteristic of the M–N stretching frequency [9,17] suggest that the glycinate ligand, –OOC–CH_2H_2N–, is co-ordinated to the metal ions via both the oxygen of the carboxylato group and the nitrogen of the amino group. This mode of co-ordination would result in the transfer of electron density from the N-atom to the metal ion causing a contrasting pull along the O–M and N-M, weakening of the M–O bond. This effect combined with the very large co-ordination geometry is expected to destabilise the ring system and the metal peroxo bonds resulting in the explosive decomposition. All Mo complexes in Group B display an interesting decomposition pathway of undergoing strongly exothermic, high activation energy reactions. This unique property may find useful application of these complexes as temperature calibrants in thermogravimetry [18].

Group C: $K_2[MO(O_2)_2(asp)]\cdot 2H_2O$ (13 and 14); $K_2[MO(O_2)_2(glu)]\cdot 2H_2O$ (15 and 16); $K_2[MO_2(O_2)_4(nicH)]\cdot H_2O$ (17 and 18); $K_2[M_2O_2(O_2)_4(nicO)]\cdot H_2O$ (19 and 20) and $K_2[MO(O_2)_2(dipic)]\cdot H_2O$ (23 and 24).

All the complexes in this group undergo initial decomposition through the loss of outer sphere water molecule(s) followed by multistage decomposition with the increasing temperature as confirmed by various thermograms. Decomposition product of complexes in this group being extremely unstable attempts to identify the true nature of the products became unsuccessful. For example the Mo-aspartate complex (13) undergoes rapid and highly exothermic decomposition ($\Delta H = -920 \pm 15\,kJ\,mol^{-1}$) without the formation of any stable intermediates as evident from the TG and DTG (see Fig. 2) and the DSC (see Fig. 4d) curves. Analysis of the residual solid at 240–250 °C showed no peroxide but a very much lower nitrogen content, 2.74% compared to 3.18% in the pure sample. This is an indication that the decomposition results from the decay of the peroxo species rather than the organic ligand. Infrared spectra of the product confirmed the presence of two peaks at 926 and 901 cm^{-1} which are characteristic of the M=O stretch suggesting the formation of an Mo-oxo species with out any peroxide. From the TG curve of wt.% loss versus temperature as shown in Fig. 5, it is evident that the W-analogue (14) also behaves in a similar manner losing the peroxide completely on heating.

TG and the DTG plots indicate that the first stage of decomposition of the Mo-glutamate (15) occurs at 50–100 °C through the gradual loss of the co-ordinated water molecules. This is evident from the ir spectra of the sample collected at 95 °C which showed no characteristic –OH absorption in the region 3200–3600 cm^{-1}. Elemental analysis of the product of 15 when heated at 150–155 °C found to be very inconsistent suggesting the formation of a highly unstable intermediate.

No peroxide was detected in this product either by elemental analysis or by the ir spectra, however, the latter did confirm the presence of a metal-oxo stretch observed at 892 cm^{-1}. For the W-analogue (16), a similar decomposition pattern was observed in the TG curve of wt.% loss versus temperature. When the compound 16 was heated isothermally to 190–200 °C for 15–20 min produced a dark brown sticky solid which contained 56.78% W. The suggestion that the sticky residue is a hydrated oxo species, $K_2[WO_3]\cdot 0.5H_2O$ finds support from the closeness of W content which requires % W = 57.22 as well as the presence of ν(W=O) at 945 and 899 cm^{-1} and the ν(OH) at 3200–3600 cm^{-1}.

From the TG and the DTG curves, it is seen that the nicH complex of Mo (17) undergoes multistage decomposition which starts just over 60 °C. Elemental analysis of the product at 105–110 °C confirmed that complex 17 suffers substantial losses of C, H and N which were found to be 6.08, 1.09 and 1.09%, respectively compared to the corresponding values of 11.88, 1.34 and 2.95% in the pure complex. Presence of the $–CO_2M$ group in the decomposition product was confirmed by a weak ir band observed at 1617cm^{-1}. However, these data do not provide sufficient clue to the exact nature of this product. W-analogue (18) also follow the similar decomposition pattern as evident from the TG plot of wt.% loss versus temperature.

Unlike the complex 17 which changed colour from yellow to orange at ∼90 °C complex 18 did, however, retain its white colour up to 180 °C which changed to light brown only above this temperature. From the analytical evidence it is suggested that the light brown solid is an oxo-tungstate, $K_2[WO_3]$ (found: %K, 25.03; %W, 59.12 and the corresponding required values for $K_2[WO_3]$ are 25.14 and 59.11%, respectively). The presence of M=O vibration frequencies observed at 933 and 844 cm^{-1} also confirms this formulation. From the TG and DTG curve, it is apparent that the nicotinic oxide complex of Mo (19) decomposes in a manner similar to that of the nicotinic acid complex (17). The decomposition of 20, however, is unique in that it forms an intermediate at 100–140 °C which is relatively stable. This intermediate when subjected to higher temperatures undergoes multistage decomposition giving products which are extremely unstable. Analytical data in Table 2c combined with the evidence from the TG and the DTG plot it is apparent that the during the initial stages of decomposition this complex suffers a steady loss of the active oxygen with increasing temperature. Although the ir spectra of this product shows the presence of a peak at 1622 cm^{-1}, characteristic of $\nu(CO_2M)$ analytical results are not conclusive enough to suggest a definite composition for this intermediate. Decomposition of the corresponding W-analogue (20) although behaves similarly as that of 19 except that no stable intermediates were formed at any stage during the decomposition process. A sample of 20 when heated in the temperature region 195–200 °C shows W content of 59.62% compared to 48.87% in the pure sample. This may be an indication that this complex itself suffers almost total destruction of the co-ordination sphere at elevated temperature. For the Mo-dipicolinate complex (23), TG and DTG plot suggest that the decomposition is a two stage process, occurring first at 40–130 °C and then at temperature >160 °C. When 23 is heated up to 153 °C there is the mass loss of 7.51% which is equivalent to the total loss of the co-ordinated H_2O molecule and possibly one molecule of active oxygen forming a species with uncertain composition. This product do retain some peroxide as evident from the chemical analysis (%O_2^{2-}, 1.72%) and a weak peak at 871 cm^{-1}. Infrared spectrum also shows a peak at 1724 cm^{-1}, characteristic of C=O vibration and this was not present in the pure sample. It may, therefore, be suggested here that the ligand pyridine-2,6-dicarboxylate itself undergoes some decomposition giving rise to a species containing the carbonyl group. The W-analogue (24) on the other hand decomposes at 120–150 °C forming an intermediate which is fairly stable. An off-white solid product is obtained after heating 24 to 130–135 °C was found to contain only 3% peroxide. The ir spectrum shows the presence of two peaks in this product observed at 1630 and 1730 cm^{-1} which are characteristics of $\nu_{sym}(CO_2M)$ and ν(C=O), respectively. Although these evidence strongly suggests that the ligand dipicolinate is still co-ordinated to the metal ion. Available analytical data in Table 2c do not point to a definite conclusion as to the identity of these products.

Apart from the observed initial mass loss, which is associated with the loss of co-ordinated H_2O molecule(s), these complexes undergo a steady and continuous decomposition route that is accompanied by the formation of highly unstable intermediates. Similar to the argument presented for Group B complexes, this behaviour can also be explained in terms of the nature of the co-ordinated organic ligands. For example, the aspartate, –OOC–CH_2–CH(NH_2)–COO– and the glutamate, –OOC–(CH_2)$_2$–CH(NH_2) –COO– presence of α-amino group in both results in the reduced stability of the M–O bonds in these complexes. The observed steady decomposition with the increasing temperature is the likely consequence of the reduced withdrawal of electron density along the M–O and the M–O_2 bonds. This theory is supported by the thermal behaviour of the aspartate and the maleate systems which have the common stoichiometry, $K_2[MO(O_2)_2(L)]\cdot 2H_2O$ with the same co-ordinate geometry. The aspartate system having an α-amino group undergoes steady decomposition without the formation of any stable intermediates. By contrast, the maleate system with a hydroxyl group is stable up to 160 °C and above which a highly explosive decomposition occurs. It is, therefore, obvious that the ligands with electron withdrawing or electron donating potential functional groups play an important role in determining the decomposition mode or the overall thermal stability of the metal peroxo complexes. Chelating oxygen-donor ligands with no electron withdrawing functional groups such as the oxalato or the citrato complexes follow a well defined decomposition route

via the formation of stable intermediates. Introduction of the substutients containing highly electronegative atoms such as O or N results in the formation of complexes that undergo highly exothermic and often explosive decomposition. It is, therefore, logical to assume that the nature of substituents coupled with the size of the central metal ion and not the co-ordination geometry of the peroxo complexes that determine the decomposition route. For example, the maleate complex $K_2[MoO(O_2)_2(malc)]\cdot 2H_2O$ decompose explosively at the highest temperature giving rise to the stable oxide $K_2[MoO_4]$, whereas the aspartate system $K_2[MoO(O_2)_2(asp)]\cdot 2H_2O$, decompose through the formation of highly unstable intermediates.

Due to limited resources number of important areas such as the detailed analyses including those of the gaseous products in the decomposition process remained poorly answered. We intend to tackle this problem in the next phase of our investigation. We also intend to extend the scope of the study to include as many transition elements as possible. There is also the need for the structural studies which may lead to much better understanding of this important aspect of chemistry.

Acknowledgements

We wish to thank the UFH for the financial assistance and Professor M.E. Brown of Rhodes University, Grahamstown for assisting with the TG, DTG and DSC analyses and Mr. H. Lachman of CSIR (Pretoria) for all microanalytical works.

References

[1] W.P. Griffith, A.C. Dengel, R.D. Powell, A.C. Skapski, J. Chem. Soc., Dalton Trans. (1987) 991–995.
[2] C. Djordjevic, B.C. Puryear, N. Vuletic, C.J. Abelt, S.J. Sheffield, Inorg. Chem. 27 (1988) 2926–2932.
[3] A.I. Vogel, A Text Book of Quantitative Inorganic Analysis, Vol. 3E, Longman, NY, 1975, (3a) pp. 256–257 and (3b) 363.
[4] H. Mimoun, in: S. Patai (Ed.), The Chemistry of Peroxides, Wiley, NY, 1983, pp. 463–482.
[5] W.P. Griffith, T.D. Wilkins, J. Chem. Soc. A (1968) 397.
[6] C. Djordjevic, S.A. Craig, E. Sinn, Inorg. Chem. 24 (1985) 1281–1283.
[7] W.P. Griffith, N.J. Campbell, C.J. Edwards, J. Chem. Soc., Dalton Trans. (1989) 1203–1208.
[8] J. Sala-Pala, J.E. Guerchais, J. Chem. Soc. A (1971) 1132–1136.
[9] K. Nakamoto, Infrared Spectra of Inorganic and Compounds, Vol. 2E, Wiley, NY, 1970.
[10] K.E. Liu, D. Wang, B.H. Huynh, D.E. Edmondson, A. Salifoglou, S.J. Lippard, J. Am. Chem. Soc. 116 (1994) 7465–7465.
[11] S.P. Goel, P.N. Mehrotra, Thermochim. Acta 68 (1983) 137–143.
[12] S.P. Goel, N.P. Mehrotra, Thermochim. Acta 70 (1983) 201–209.
[13] F.A. Cotton, G. Wilkinson, Advanced Inorganic Chemistry, Vol. 5E, Wiley, NY, 1988, pp. 468–470, 827–831.
[14] A. Beltran-Porter, E. Tamayo, F. Caturla, Thermochim. Acta 75 (1984) 303–311.
[15] A.L. Feig, M. Bekar, S. Schindler, R. van Eldik, S.J. Lippard, Inorg. Chem. 35 (1996) 2590–2601.
[16] M. Kodera, Y. Taniika, M. Itoh, Y. Tanahashi, H. Shimakosi, K. Kano, S. Hirota, S. Iijima, M. Ohba, H. Okawa, Inorg. Chem. 40 (2001) 4821–4822.
[17] P.J. Hendra, B.A. Sadasivan, Spectrochim. Acta 21 (1965) 1271.
[18] M.E. Brown, T.T. Bhengu, D.K. Sanyal, Thermochim. Acta 242 (1994) 141–145.